JCS–Japan

TECHNICAL REPORT

Reassessment of vibration spectra in alkaline earth metaphosphate crystals

Jun Endo[1] and Yoshikazu Suzuki[1,2,†]

[1] Graduate School of Science and Technology, University of Tsukuba, 1–1–1 Tennodai, Tsukuba, Ibaraki 305–8573, Japan
[2] Faculty of Pure and Applied Sciences, University of Tsukuba, 1–1–1 Tennodai, Tsukuba, Ibaraki 305–8573, Japan

The Raman and infrared (IR) spectra for the alkaline earth metaphosphate crystals with chains were assessed by density functional theory (DFT) calculations. The assignments of peaks of the DFT calculated Raman and IR spectra were consistent with reported assignments of phosphate crystals and glasses except for the assignment of the peaks around $1100\,cm^{-1}$ of the calculated IR spectra. Peaks around $1100\,cm^{-1}$ of IR spectra for phosphate crystals and glasses have been assigned to asymmetric stretching vibrations of bonds between phosphorus atoms and non-bridging oxygens (NBO) of Q^1 units. However, the calculated IR spectra showed that symmetric stretching vibrations of P–NBO bonds and asymmetric stretching vibrations of –P–O–P– bonds of Q^2 units also result in peaks around $1100\,cm^{-1}$. In addition, the calculated Raman spectra showed a strong correlation between cation field strength and the Raman shift of intense peaks assigned to symmetric stretching vibrations of P–NBO bonds of Q^2 units.
©2022 The Ceramic Society of Japan. All rights reserved.

Key-words : Alkaline earth metaphosphate crystal, Raman spectrum, IR spectrum, Density functional theory, DFT, Quantum ESPRESSO

1. Introduction

Phosphate glasses have been studied for a wide range of applications such as alkaline earth phosphate glasses for bioactive materials and rare-earth ion host materials for laser.[1]–[4] Phosphate glasses are composed of PO_4 tetrahedral units, which are called Q^n units depending on the number of bridging oxygen atoms n ($n = 0$–3). Q^2 units form –P–O–P– chains and rings by linking each other with two covalent bonds. Metaphosphate glasses are mainly composed of Q^2 units, but also contain Q^1 units.[5]–[9] Structures of phosphate glasses were investigated by analyzing NMR, Raman, and infrared (IR) spectra.[5]–[9] The relationships between structure and peak wavenumbers of IR spectra of phosphate crystals were used for peak assignments of IR spectra for phosphate glasses.[10],[11] Peaks around $1100\,cm^{-1}$ of IR spectra for phosphate crystals and glasses have been assigned to asymmetric stretching vibrations of bonds between phosphorus atoms and non-bridging oxygens (NBO) of Q^1 units [$\nu_{as}(PO_3^{2-})$].[6]–[10]

Recently, we have reported that calculated IR spectra of alkali metaphosphate crystals with chains composed of Q^2 units (i.e., $LiPO_3$, $NaPO_3$, and KPO_3) and pyrophosphate crystal composed of Q^1 units (i.e., $Na_4P_2O_7$) showed that the peaks around $1100\,cm^{-1}$ result from not only

$\nu_{as}(PO_3^{2-})$ but also symmetric stretching vibrations of P–NBO bonds [$\nu_s(PO_2^{-})$] and asymmetric stretching vibrations of –P–O–P– bonds [$\nu_{as}(P–O–P)$] of Q^2 units.[12]

In this study, we have then investigated vibration modes of alkaline earth metaphosphate crystals with chains [i.e., $Ca(PO_3)_2$, $Sr(PO_3)_2$, and $Ba(PO_3)_2$] by density functional theory (DFT) calculations of Raman and IR spectra to verify the interpretations of peak assignments reported in previous studies. In addition, the structural key factors which have a significant effect on compositional dependence of Raman shift were investigated.

2. Experimental

Calculations of plane wave DFT of $50CaO$–$50P_2O_5$ [in mol %, $Ca(PO_3)_2$], $50SrO$–$50P_2O_5$ [in mol %, $Sr(PO_3)_2$], and $50BaO$–$50P_2O_5$ [in mol %, $Ba(PO_3)_2$] metaphosphate crystals with chains were performed using the Quantum ESPRESSO (Ver. 6.6) package.[13],[14] The exchange–correlation functional of the local density approximation was used. Pseudopotentials were norm-conserving scalar relativistic types. The pseudopotentials are listed in the pseudopotential table at http://www.pseudo-dojo.org.[15],[16] The plane-wave energy cutoffs for the wave functions (ecutwfc) and the charge density (ecutrho) were set at 150 Rydberg and 600 Rydberg (4 × ecutwfc), respectively. The k-point mesh was 2 × 2 × 2. A structure relaxation including optimization of the lattice parameters and the atomic positions in a cell with keeping the Bravais lattice

† Corresponding author: Y. Suzuki; E-mail: suzuki@ims. tsukuba.ac.jp

of experimental crystals[17]–[19] was carried out. **Figure 1** shows a relaxed structure of $Sr(PO_3)_2$ crystal with chains.[18] Raman and IR spectra were calculated using the relaxed structures. Deviations of lattice parameters between the experimental and relaxed structures were equal to or less than 2.2 % as shown in **Table 1**. The calculated spectra were analyzed using Winmostar Ver. 10.5.4 software (X-Ability Co., Ltd., Japan).

3.   Results and discussion

Figure 2 shows the calculated Raman and IR spectra for the alkaline earth metaphosphate crystals with chains. The assignment of peaks of the calculated spectra is listed in **Table 2**.

Three or four peaks were observed in the Raman spectra of the alkaline earth metaphosphate crystals. The peaks around $680\,cm^{-1}$ were assigned to symmetric stretching vibrations of –P–O–P– bonds [ν_s(P–O–P)]. The peaks around $1150\,cm^{-1}$ were assigned to symmetric stretching vibrations of P–NBO bonds of Q^2 units [ν_s(PO$_2^-$)]. The peaks in the range 1220–$1280\,cm^{-1}$ were assigned to asymmetric stretching vibrations of P–NBO bonds of Q^2 units [ν_{as}(PO$_2^-$)].
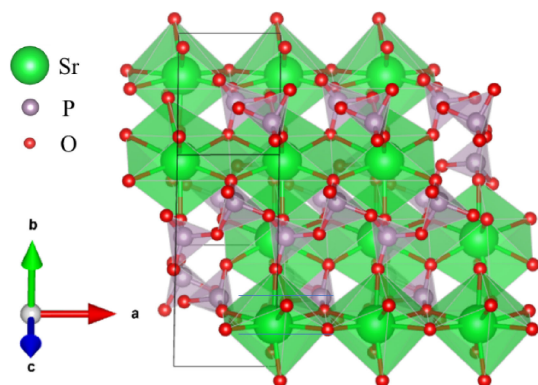

Fig. 1.   Structure of $Sr(PO_3)_2$ metaphosphate crystal with chains.[18]

Seven or Nine peaks were observed in the IR spectra of the alkaline earth metaphosphate crystals. The peaks in the range 668–$784\,cm^{-1}$ were assigned to symmetric stretching vibrations of –P–O–P– bonds [ν_s(P–O–P)]. The peaks in the range 860–$936\,cm^{-1}$ were assigned to asymmetric stretching vibrations of –P–O–P– bonds [ν_{as}(P–O–P)]. The peaks in the range 1005–$1107\,cm^{-1}$ were assigned to symmetric stretching vibrations of P–NBO bonds [ν_s(PO$_2^-$)] and asymmetric stretching vibrations of –P–O–P– bonds [ν_{as}(P–O–P)]. The peaks in the range 1193–$1299\,cm^{-1}$ were assigned to asymmetric stretching vibrations of P–NBO bonds of Q^2 units [ν_{as}(PO$_2^-$)].

Reported peak assignment of Raman and IR spectra for phosphate crystals and glasses, and peak assignment of calculated Raman and IR spectra for alkali metaphosphate crystals with chains in our previous study are also listed in

Table 1. Lattice parameters of experimental[17]–[19] and relaxed structures of $Ca(PO_3)_2$, $Sr(PO_3)_2$, and $Ba(PO_3)_2$ metaphosphate crystals with chains

Crystal	Lattice parameters	Experimental structure	Relaxed structure	Deviation (%)
$Ca(PO_3)_2$	a (Å)	16.960	16.703	−1.5
	b (Å)	7.714	7.620	−1.2
	c (Å)	6.996	6.847	−2.1
	α (°)	90.000	90.000	0.0
	β (°)	90.394	90.316	−0.1
	γ (°)	90.000	90.000	0.0
$Sr(PO_3)_2$	a (Å)	4.498	4.432	−1.5
	b (Å)	10.911	10.672	−2.2
	c (Å)	10.375	10.233	−1.4
	α (°)	90.000	90.000	0.0
	β (°)	91.560	91.836	0.3
	γ (°)	90.000	90.000	0.0
$Ba(PO_3)_2$	a (Å)	4.498	4.438	−1.3
	b (Å)	8.338	8.170	−2.0
	c (Å)	13.391	13.096	−2.2
	α (°)	90.000	90.000	0.0
	β (°)	90.000	90.000	0.0
	γ (°)	90.000	90.000	0.0
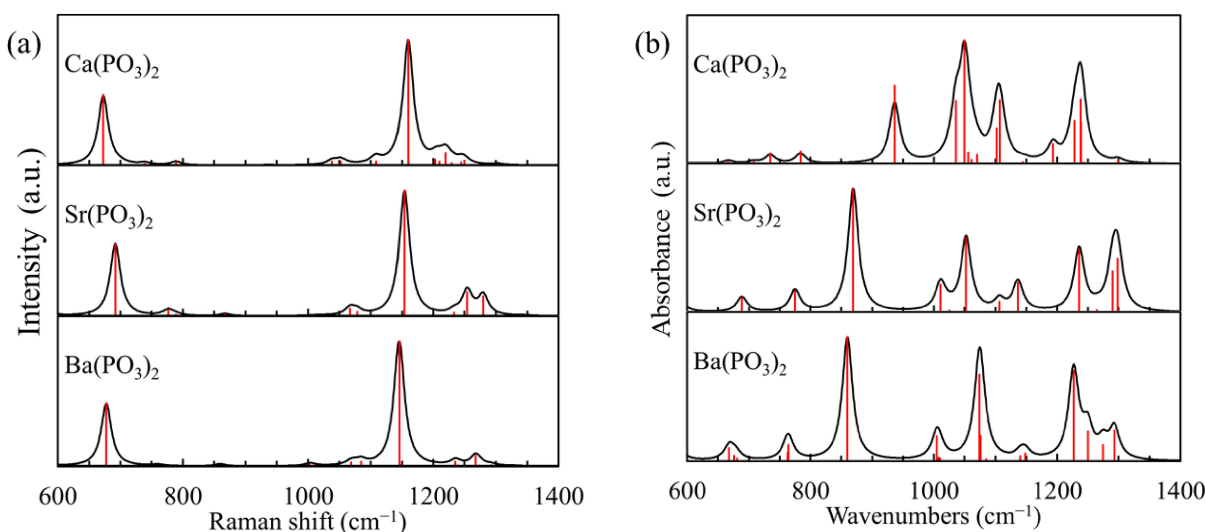
Fig. 2.   Calculated (a) Raman and (b) IR spectra of $Ca(PO_3)_2$, $Sr(PO_3)_2$, and $Ba(PO_3)_2$ metaphosphate crystals with chains.

Table 2. Peak assignment of calculated Raman and IR spectra for Ca(PO$_3$)$_2$, Sr(PO$_3$)$_2$, and Ba(PO$_3$)$_2$ metaphosphate crystals with chains, and peak assignment of calculated Raman and IR spectra for 50Li$_2$O–50P$_2$O$_5$ (in mol %, LiPO$_3$), 50Na$_2$O–50P$_2$O$_5$ (in mol %, NaPO$_3$), and 50K$_2$O–50P$_2$O$_5$ (in mol %, KPO$_3$) metaphosphate crystals with chains,[12] and reported peak assignment of Raman and IR spectra of phosphate crystals and glasses.[6]–[10] ν_s and ν_{as} in the assignment are symmetric and asymmetric stretching vibrations, respectively

Ca(PO$_3$)$_2$ crystal with chain		Sr(PO$_3$)$_2$ crystal with chain		Ba(PO$_3$)$_2$ crystal with chain		LiPO$_3$, NaPO$_3$, KPO$_3$ crystals with chain[12]			Phosphate glasses and crystals[6]–[10]		
Raman (cm^{-1})	IR (cm^{-1})	Raman (cm^{-1})	IR (cm^{-1})	Raman (cm^{-1})	IR (cm^{-1})	Raman (cm^{-1})	IR (cm^{-1})	Assignment	Raman (cm^{-1})	IR (cm^{-1})	Assignment
673	734	692	689	678	668	674 −686	676 −725 764 −791	ν_s(P–O–P), Q^2 units	635 −835	650 −850	ν_s(P–O–P), Q^2 units
	784		775		764						
	936		869		860		881 −929 1011 −1032	ν_{as}(P–O–P), Q^2 units		850 −1055	ν_{as}(P–O–P), Q^2 units
	1050 1107		1011 1052 1107		1005 1074		1099 −1125	ν_s(PO$_2^-$) and ν_{as}(P–O–P), Q^2 units	Not reported	Not reported	Not Reported
1160		1154	1137	1145		1165 −1184	1148 −1174	ν_s(PO$_2^-$), Q^2 units	1134 −1245	1134 −1245	ν_s(PO$_2^-$), Q^2 units
1220	1193 1238	1254	1236 1280 1299	1268	1227 1293	1273 −1335	1284 −1319	ν_{as}(PO$_2^-$), Q^2 units	1167 −1286	1194 −1293	ν_{as}(PO$_2^-$), Q^2 units

Table 3. Raman shift of intense peaks of calculated Raman spectra, average bond length, and average bond angle for Ca(PO$_3$)$_2$, Sr(PO$_3$)$_2$, and Ba(PO$_3$)$_2$ metaphosphate crystals

Crystal	Ca(PO$_3$)$_2$	Sr(PO$_3$)$_2$	Ba(PO$_3$)$_2$
Raman shift of intense peaks (cm^{-1})	673 1160	692 1154	678 1145
Average length of P–BO bond (Å)	1.581	1.602	1.606
Average angle of P–BO–P bond (°)	138.0	125.7	127.5
Average length of P–NBO bond (Å)	1.485	1.480	1.480
Average length of M–NBO bond (Å)	2.412	2.557	2.827
Average angle of NBO–P–NBO bond (°)	117.5	120.3	119.5

Fig. 3. Relationship between Raman shift of intense peaks of calculated Raman spectra around 1150 cm^{-1} and field strength (F) for Ca(PO$_3$)$_2$, Sr(PO$_3$)$_2$, and Ba(PO$_3$)$_2$ metaphosphate crystals with chains. Dash line is a regression line. R^2 is the determination coefficient.

Table 2.[6]–[10],[12] The peak assignments of the calculated Raman and IR spectra for the alkaline earth metaphosphate crystals were consistent with reported peak assignments for phosphate crystals and glasses except for the assignment of the peaks around 1100 cm^{-1} of the calculated IR spectra.

The peaks around 1100 cm^{-1} of the calculated IR spectra for the alkaline earth metaphosphate crystals were assigned to ν_s(PO$_2^-$) and ν_{as}(P–O–P) in this study. The peak assignments for the alkaline earth metaphosphate crystals with chains in this study were the same as those for the alkali metaphosphate crystals with chains in our previous study.

Table 3 shows the Raman shift of intense peaks of the calculated Raman spectra, bond length, and bond angle for the alkaline earth metaphosphate crystals. A clear correlation between the Raman shift of intense peaks around 680 cm^{-1} and crystal structure, i.e. average length of P–
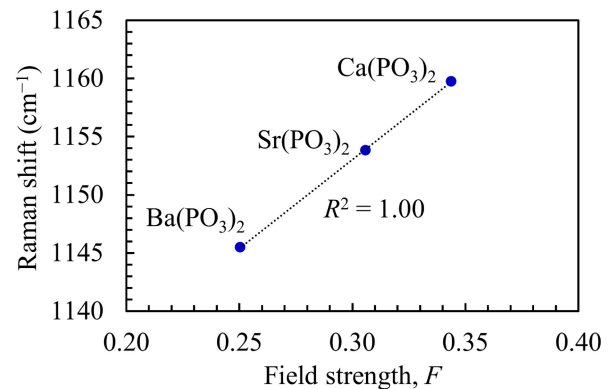
BO bond and the average angle of P–BO–P bond was not observed (BO is bridging oxygen). On the other hand, the Raman shift of intense peaks around 1150 cm^{-1} decreased with increasing average length of M–NBO bond (M is alkaline earth cation). Field strength (F) of a cation is defined by the following equation:

$$F = \frac{Z_{cation}}{(r_{cation} + r_{oxygen})^2}$$

where Z_{cation} is the valence of cation, and r_{cation} and r_{oxygen}, respectively, are ionic radii of cation and oxygen ions in Å unit.[20] **Figure 3** shows the relationship between Raman shift of intense peak around 1150 cm^{-1} and field strength for the alkaline earth metaphosphate crystals. The field strength was calculated by using $Z_{cation} = 2$ and the average length of M–NBO bond shown in Table 3, which is

equal to $r_{cation} + r_{oxygen}$. The Raman shift of intense peaks around 1150 cm^{-1} increased with increasing field strength. Linear relationship and a strong correlation between the field strength and the Raman shift of intense peaks around 1150 cm^{-1} was observed because determination coefficient (R^2) was 1.00. Since chains in alkaline earth metaphosphate crystals are connected by cross-link of alkaline earth cations, the larger Raman shift of intense peak of calculated Raman spectra around 1150 cm^{-1} for Ca(PO$_3$)$_2$ crystal compared to Sr(PO$_3$)$_2$ and Ba(PO$_3$)$_2$ crystals reflects stronger cross-link between chains for Ca(PO$_3$)$_2$ crystal compared to Sr(PO$_3$)$_2$ and Ba(PO$_3$)$_2$ crystals.

4. Conclusions

The Raman and IR spectra for Ca(PO$_3$)$_2$, Sr(PO$_3$)$_2$, and Ba(PO$_3$)$_2$ metaphosphate crystals with chains were assessed by DFT calculations. The assignments of peaks of the calculated Raman and IR spectra were consistent with reported assignments of phosphate crystals and glasses except for the assignment of the peaks around 1100 cm^{-1} of the calculated IR spectra. Peaks around 1100 cm^{-1} of IR spectra for phosphate crystals and glasses have been assigned to asymmetric stretching vibrations of P–NBO bonds of Q^1 units. However, the calculated IR spectra showed that symmetric stretching vibrations of P–NBO bonds and asymmetric stretching vibrations of –P–O–P– bonds of Q^2 units also result in peaks around 1100 cm^{-1}.

The peak assignments for the alkaline earth metaphosphate crystals with chains in this study were the same as those for the alkali metaphosphate crystals with chains in our previous study. In addition, the calculated Raman spectra showed a linear relationship and strong correlation between cation field strength and the Raman shift of intense peaks assigned to symmetric stretching vibrations of P–NBO bonds of Q^2 units. The larger Raman shift of calculated Raman spectra around 1150 cm^{-1} for Ca(PO$_3$)$_2$ crystal compared to Sr(PO$_3$)$_2$ and Ba(PO$_3$)$_2$ crystals reflects stronger cross-link between chains for Ca(PO$_3$)$_2$ crystal compared to Sr(PO$_3$)$_2$ and Ba(PO$_3$)$_2$ crystals.

References

1) A. Matamoros-Veloza, K. M. Z. Hossain, B. E. Scammell, I. Ahmed, R. Hall and N. Kapur, *J. Mech. Behav. Biomed.*, **102**, 103489 (2020).
2) R. M. Pilliar, M. J. Filiaggi, J. D. Wells, M. D. Grynpas and R. A. Kandel, *Biomaterials*, **22**, 963–972 (2001).
3) A. Speghini, R. Francini, A. Martinez, M. Tavernese and M. Bettinelli, *Spectrochim. Acta A*, **57**, 2001–2008 (2001).
4) Z. Mazurak, S. Bodył, R. Lisiecki, J. Gabryś-Pisarska and M. Czaja, *Opt. Mater.*, **32**, 547–553 (2010).
5) R. K. Brow, R. J. Kirkpatrick and G. L. Turner, *J. Non-Cryst. Solids*, **116**, 39–45 (1990).
6) K. Griebenow, U. Hoppe, D. Möncke, E. I. Kamitsos and L. Wondraczek, *J. Non-Cryst. Solids*, **460**, 136–145 (2017).
7) L. L. Velli, C. P. E. Varsamis, E. I. Kamitsos, D. Möncke and D. Ehrt, *Phys. Chem. Glasses*, **46**, 178–181 (2005).
8) K. Griebenow, C. B. Bragatto, E. I. Kamitsos and L. Wondraczek, *J. Non-Cryst. Solids*, **481**, 447–456 (2018).
9) G. L. Saoût, P. Simon, F. Fayon, A. Blin and Y. Vaills, *J. Raman Spectrosc.*, **33**, 740–746 (2002).
10) A. Rulmont, R. Cahay, M. Liegeois-Duychaerts and P. Tarte, *Eur. J. Sol. State Inor.*, **28**, 207–219 (1991).
11) E. I. Kamitsos, J. A. Kapoutsis, G. D. Chryssikos, J. M. Hutchinson, A. J. Pappin, M. D. Ingram and J. A. Duffy, *Phys. Chem. Glasses*, **36**, 141–149 (1995).
12) J. Endo and Y. Suzuki, *J. Ceram. Soc. Jpn.*, **130**, 324–326 (2022).
13) P. Giannozzi, S. Baroni, N. Bonini, M. Calandra, R. Car, C. Cavazzoni, D. Ceresoli, G. L. Chiarotti, M. Cococcioni, I. Dabo, A. D. Corso, S. de Gironcoli, S. Fabris, G. Fratesi, R. Gebauer, U. Gerstmann, C. Gougoussis, A. Kokalj, M. Lazzeri, L. Martin-Samos, N. Marzari, F. Mauri, R. Mazzarello, S. Paolini, A. Pasquarello, L. Paulatto, C. Sbraccia, S. Scandolo, G. Sclauzero, A. P. Seitsonen, A. Smogunov, P. Umari and R. M. Wentzcovitc, *J. Phys.-Condens. Mat.*, **21**, 395502 (2009).
14) P. Giannozzi, O. Andreussi, T. Brumme, O. Bunau, M. Buongiorno Nardelli, M. Calandra, R. Car, C. Cavazzoni, D. Ceresoli, M. Cococcioni, N. Colonna, I. Carnimeo, A. Dal Corso, S. de Gironcoli, P. Delugas, R. A. DiStasio, Jr., A. Ferretti, A. Floris, G. Fratesi, G. Fugallo, R. Gebauer, U. Gerstmann, F. Giustino, T. Gorni, J. Jia, M. Kawamura, H.-Y. Ko, A. Kokalj, E. Küçükbenli, M. Lazzeri, M. Marsili, N. Marzari, F. Mauri, N. L. Nguyen, H.-V. Nguyen, A. Otero-de-la-Roza, L. Paulatto, S. Poncé, D. Rocca, R. Sabatini, B. Santra, M. Schlipf, A. P. Seitsonen, A. Smogunov, I. Timrov, T. Thonhauser, P. Umari, N. Vast, X. Wu and S. Baroni, *J. Phys.-Condens. Mat.*, **29**, 465901 (2017).
15) M. J. van Setten, M. Giantomassi, E. Bousquet, M. J. Verstraete, D. R. Hamann, X. Gonze and G.-M. Rignanese, *Comput. Phys. Commun.*, **226**, 39–54 (2018).
16) D. R. Hamann, *Phys. Rev. B*, **88**, 085117 (2013).
17) M. Schneider, K. H. Jost and P. Leibnitz, *Z. Anorg. Allg. Chem.*, **527**, 99–104 (1985).
18) M. Graia, A. Driss and T. Jouini, *Acta Crystallogr. C*, **55**, 1395–1398 (1999).
19) M. Weil, *Acta Crystallogr. E*, **70**, i7 (2014).
20) A. Dietzel, *Z. Elektrochem.*, **48**, 9–23 (1942).
21) K. Momma and F. Izumi, *J. Appl. Crystallogr.*, **44**, 1272–1276 (2011).